

The sizes of mini-voids in the local universe: an argument in favor of a warm dark matter model?

A. V. Tikhonov^{1*}, S. Gottlöber^{2†}, G. Yepes^{3‡} and Y. Hoffman^{4§}

¹*Saint Petersburg State University, Russian Federation*

²*Astrophysical Institute Potsdam, An der Sternwarte 16, 14482 Potsdam, Germany*

³*Universidad Autónoma de Madrid, Grupo de Astrofísica, 28049 Madrid, Spain*

⁴*Racah Institute of Physics, Hebrew University, Jerusalem 91904, Israel*

ABSTRACT

Using high-resolution simulations within the Cold and Warm Dark Matter models we study the evolution of small scale structure in the Local Volume, a sphere of 8 Mpc radius around the Local Group. We compare the observed spectrum of mini-voids in the Local Volume with the spectrum of mini-voids determined from the simulations. We show that the Λ WDM model can easily explain both the observed spectrum of mini-voids and the presence of low-mass galaxies observed in the Local Volume, provided that all haloes with circular velocities greater than 20 km/s host galaxies. On the contrary within the Λ CDM model the distribution of the simulated mini-voids reflects the observed one if haloes with maximal circular velocities larger than 35 km s⁻¹ host galaxies. This assumption is in contradiction with observations of galaxies with circular velocities as low as 20 km/s in our Local Universe. A potential problem of the Λ WDM model could be the late formation of the haloes in which the gas can be efficiently photo-evaporated. Thus star formation is suppressed and low-mass haloes might not host any galaxy at all.

Key words: cosmology: large-scale structure of Universe, voids, dark matter, wdm paradigm ; galaxies: luminosity function, rotational velocities

1 INTRODUCTION

At present the standard model of cosmology is a flat Friedmann universe whose mass-energy content is dominated by a cosmological constant (the Λ term), a Cold Dark Matter (CDM) component and baryons. This Λ CDM model is characterized by only a few parameters which are determined already with high precision. The Λ CDM model describes structure formation at large scales very well, however it fails on small scales: the standard model predicts much more small scale structure than observed. This concerns the number of dark matter sub-haloes inside galactic-sized host haloes (Klypin et al. 1999; Moore et al. 1999) as well as the number of dwarfs in low density regions of the universe (Peebles 2001). A better understanding of the physics of structure formation on small scales, in particular of the correct modeling of baryonic physics, could solve these problems (Hoeft et al. 2006; Crain et al. 2007). How-

ever, any non-baryonic physics that reduces power on small scales compared to the standard model will also improve the situation. It is well known that warm dark matter acts in this direction by erasing power at short scales due to free streaming.

Recently Tikhonov & Klypin (2009) studied the spectrum of mini-voids in the distribution of galaxies down to $M_B = -12$ in a sphere of radius 8 Mpc around the Milky Way (the Local Volume – LV). They compared the spectrum of mini-voids obtained in LV-candidates selected in numerical simulations based on WMAP1 (Spergel et al. 2003) and WMAP3 (Spergel et al. 2007) cosmologies and concluded that it matches the observed one only if haloes with circular velocities $V_c > 35 - 40$ km/s define the mini-voids. Thus Tikhonov & Klypin (2009) conclude that Λ CDM haloes with $V_c < 35 - 40$ km/s should not host galaxies brighter than $M_B = -12$, in fairly agreement with theoretical expectations (Hoeft et al. 2006; Loeb 2008). In the LV, however, a substantial number of quite isolated galaxies has been observed with a total of regular (circular) and chaotic motions well below 35 km s⁻¹ (Begum et al. 2008). These observed galaxies point towards the same overabundance problem that the Λ CDM model has in case of Milky Way satel-

* E-mail: avtikh@gmail.com

† E-mail: sgottloeber@aip.de

‡ E-mail: gustavo.yepes@uam.es

§ E-mail: yhoffman@huji.ac.il

lites. If haloes with circular velocities $V_c < 35$ km/s would host galaxies their total number is predicted to be too large compared to data.

In Warm Dark Matter (WDM) cosmologies the number of low-mass haloes drops down when their mass is below a critical damping scale which depends on the mass of the WDM particles (see e.g. Avila-Reese et al. (2001), Bode, Ostriker, & Turok (2001), Knebe et al. (2002)). In this work, we will use high-resolution N-body simulations of different dark matter candidates, namely CDM and WDM, in order to study the properties of LVs in these models and compared with the real LV observations. In particular, we will compare the void functions in simulated "LV-candidates" with observations in order to derive possible conclusions about the nature of dark matter particles.

Unfortunately, little is known about the nature of the dark matter. One of the promising dark matter candidates is the gravitino for which three possible scenarios are imaginable: Warm (superWIMP) or mixed cold/warm or cold gravitino dark matter (Steffen 2006). Another possible candidate are sterile neutrinos which exhibit a significant primordial velocity distribution and thus damp primordial inhomogeneities on small scales (Abazajian & Koushiappas 2006). Experiments are far away from the scales which could probe directly the properties of the particles of which the dark matter is made of, so that the free streaming length cannot be predicted. However, the free streaming length can be associated with the particles mass for which astrophysical constraints can be determined.

There is a number of observational constraints on the mass of the WDM particles. Using HIRES data, a lower limit of $m_{WDM} = 1.2$ keV has been reported by Viel et al. (2008) which increases to 4.0 keV when a combination of SDSS and HIRES data was used. From the power spectrum of SDSS galaxies, a lower limit of 0.11 keV has been reported by Abazajian (2006) which also increases to 1.7 keV if the SDSS Ly α forest is considered and further increases to 3.0 keV if high-resolution Ly α forest data are taken into account. An independent estimation of lower limits for the mass of the WDM particle based on QSO lensing observations are in agreement with the former results (Miranda & Macciò 2007). Recently, Viel, Colberg, & Kim (2008) have shown that the properties of the void population seen in the Lyman α forest spectra depend on the underlying power spectrum and, therefore, these voids may also constrain the properties of the dark matter. We have run a suite of WDM simulations with particle masses ranging from 3 to 1 KeV. However, in this paper we will consider only the results from simulations done with the lighter WDM particles (1 KeV). Results from the other simulations will be reported elsewhere.

In this paper we will focus on the comparison between the observed spectrum of mini-voids in the Local Universe with the simulated ones in Λ CDM and Λ WDM models. The structure of this paper is as follows, in Section 2 we describe briefly our numerical simulations, the halo mass functions and discuss the reliability of the subsequent analysis. In Section 3 we describe the observational data sample used here. In Section 4 we discuss our void finding algorithm. In Section 5 we present results from Λ WDM and Λ CDM simulations in terms of spatial distribution and dynamics. We conclude this paper with a discussion of the results found.

2 SIMULATIONS

For our numerical experiments, we have assumed a spatially flat cosmological model which is compatible with the 3rd year WMAP data (Spergel et al. 2007) with the parameters $h = 0.73$, $\Omega_m = 0.24$, $\Omega_{bar} = 0.042$, $\Omega_\Lambda = 0.76$, the normalization $\sigma_8 = 0.75$ and the slope $n = 0.95$ of the power spectrum. A computational box of $64h^{-1}$ Mpc on a size was used for all simulations. For Λ CDM a random realization of the initial power spectrum computed from a Boltzmann code by W. Hu, was done using 4096^3 N-body particles. After applying the Zeldovich approximation to this set of particles, we reduced the particles to a total number of 1024^3 , which corresponds to a mass per particle of $1.6 \times 10^7 h^{-1} M_\odot$. We used the original displacement field on the 4096^3 mesh to derive the initial conditions (i.e positions and velocities) of the final 1024^3 particles. In this way, we can increase the mass resolution of all, or a particular area of the simulation up to 64 times more using zooming techniques. This is specially useful to study the problem of *fake* haloes in WDM (see below). The same random phases have been used in both simulation, so we ensure that the same structures will be formed in both models. The initial redshift of the simulations was set to 50 in all cases.

To generate initial conditions for WDM, we used a rescaled version of the CDM power spectrum using a fitting function that approximates the transfer function associated to the free streaming effect of WDM particles with $m_{WDM} = 1 - 3$ keV (Viel et al. 2005). The power spectra of the three models are shown in Fig. 1.

The effects of the velocity dispersion of the WDM particles have been neglected in these simulations. They would introduce a certain level of white noise in the initial conditions that would contribute to the growth of the small scale power (Colín, Valenzuela, & Avila-Reese 2008) that lead to the formation of spurious halos. At the same time, the rms value of the random velocity component for 1 keV particles at the starting redshift of the simulations ($z=50$) is of the order of 2 km/s which is much smaller than the typical velocities induced by the gravitational collapse of the minimum resolved structures in our simulation (see Zavala et al. (2009) for more details).

These simulations were run with the purpose in mind of studying the gross structures of the nearby Universe, such as the Local Supercluster (LSC) and the Virgo cluster, i.e, to use them to do Near Field Cosmology. This could be achieved by imposing linear constraints coming from observations to the otherwise Gaussian random field of density fluctuations. We used the Hoffman & Ribak (1991) algorithm for imposing the constraints on large scales. A more detailed description of the simulations and their use for doing Near Field Cosmology will be reported in a forthcoming paper (Yepes et al. 2009). However, the constrained nature of the simulations is ignored here and they are treated as standard random simulations.

The simulations have been performed using the TreePM parallel N-body code GADGET2 (Springel 2005). The spatial resolution (Plummer softening length) was set to the maximum between $1.6h^{-1}$ kpc comoving and $0.8h^{-1}$ kpc physical at all redshifts.

In an N-body simulation, the computational box size (k_F) and the number of particles (k_{Ny}) determine the fil-

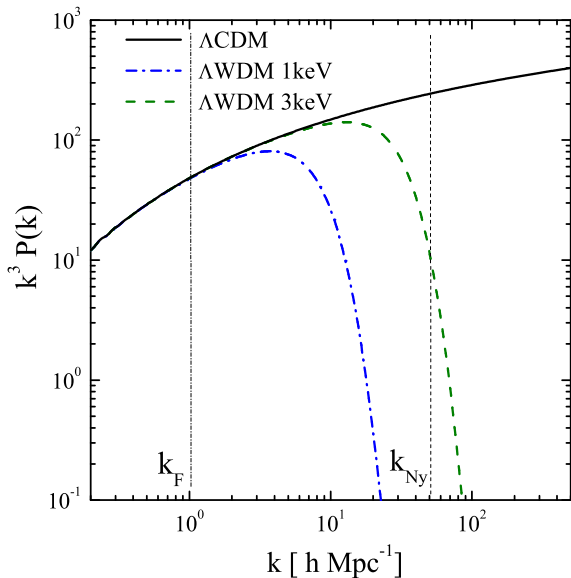


Figure 1. The dimensionless theoretical power spectra for the models considered here: CDM (black), and WDM with particle masses: 3 keV (blue), and 1 keV (red). The dotted lines correspond to the fundamental mode (box size $64h^{-1}\text{Mpc}$) and the Nyquist frequencies.

tering scales of the theoretical power spectrum. In Fig. 1 we represent these two scales for our simulations. As can be seen, the Nyquist frequency is well below the exponential cut-off in the power spectrum for WDM with $m_{WDM} = 3$ keV. Therefore, we cannot expect too much difference between the halo mass function of ΛCDM and this particular ΛWDM model, since both are dominated mainly by the lack of mass resolution. Therefore, we decided not to run the 3 keV WDM simulation at this resolution. Rather, we used it to study the excess of satellites in Milky Way type haloes, in which re-simulations of haloes with full resolution (i.e. 4096^3 particles) have been used for the 3 models (Yepes et al. 2009). Here we concentrate on the simulation with 1024^3 WDM-particles of 1 keV mass.

In order to identify haloes in the simulation we have used the AMIGA Halo Finder (AHF) (Knollmann & Knebe 2008). The halo positions are first identified from the local maxima of the density field that is computed from the particle distribution by Adaptive Mesh Refinement techniques. The AHF identifies haloes as well as sub-haloes. It provides the virial masses, virial radii and circular velocities of isolated haloes and some related quantities for sub-haloes. We use the maximum circular velocity V_c to characterize the haloes because the circular velocity can be easier related to observations than the virial mass. For reference, haloes with $V_c = 50 \text{ km s}^{-1}$ have a virial mass of about $10^{10} M_\odot$ and haloes with $V_c = 20 \text{ km s}^{-1}$ have a virial mass about $10^9 M_\odot$. We re-scaled all data (coordinates and masses of haloes) to “real” units assuming $H_0 = 72 \text{ km/s/Mpc}$, which is the value assumed by Karachentsev et al. (2004) in the ob-

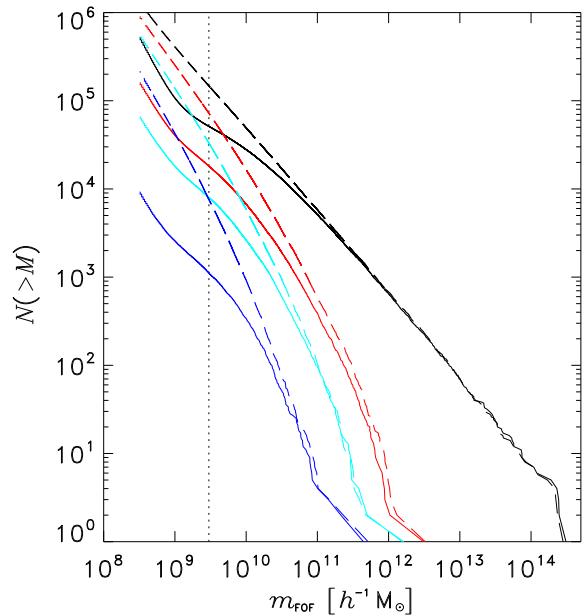


Figure 2. Cumulative FOF halo mass functions with more than 20 particles for the ΛCDM (dashed line) and ΛWDM (solid line) models. From left to right the mass functions are shown at redshifts $z = 8, 6, 5,$ and 0 . The dotted line marks $M_{\text{lim}} = 3 \times 10^9 h^{-1} M_\odot$.

served LV and which is almost identical with value assumed in the simulations ($H_0 = 73 \text{ km/s/Mpc}$)

It is known that in WDM simulations small mass haloes can arise from the artificial gravitational growth of Poissonian fluctuations that lead to an unphysical fragmentations of filaments (Wang & White 2007). These “fake” haloes show up typically as tiny haloes regularly aligned along filaments. In Figure 1 one can clearly see the exponential cut-off of power in the ΛWDM models. For the 1keV WDM model the maximum power is reached at $k_{\text{peak}} = 3.7h\text{Mpc}^{-1}$. Above this wave number the linear power spectrum contains very little power so that discreteness noise influences the growth of small-scale non-linear structures. Below a characteristic mass M_{lim} , which depends on the mass resolution in the simulation, a spurious fragmentation of filaments occurs which leads to an upturn of the halo mass function at small scales (Fig. 2). Following Wang & White (2007) we have estimated for our simulations this limiting mass as $M_{\text{lim}} \approx 3 \times 10^9 h^{-1} M_\odot$.

Figure 2 shows the evolution of the cumulative mass functions of haloes found by the friend-of-friends algorithm in the ΛCDM and ΛWDM simulations. The upturn of the ΛWDM mass function can be seen at any redshift between $z = 8$ and $z = 0$ and it is always at the same position slightly left of the limiting mass. The dotted line marks the limiting mass $3 \times 10^9 h^{-1} M_\odot$ for $z = 0$. This points to a complex process of the formation of spurious fake-haloes. It seems that they do not form only at a certain epoch but instead appear all the time after the formation of the first haloes. A more detailed numerical study of this problem is definitively needed, but it is outside of the scope of the present paper.

Since we see an upturn of the mass function only at $\approx 1 \times 10^9 h^{-1} M_\odot$ we consider M_{lim} as a rather conservative value. In terms of circular velocity M_{upturn} corresponds to haloes with $V_{\text{max}} \lesssim 20 \text{ km/s}$ which are candidates to be spurious. The prime objective of the paper is the study of the statistical properties of voids, and it is therefore important to establish that these are not affected by the spurious halos. Figure 5 below proves that this is indeed the case.

3 OBSERVATIONAL DATA: LOCAL VOLUME

Over the last decade Hubble Space Telescope observations have provided distances to many nearby galaxies which were measured with the tip of the Red Giant Branch (TRGB) stars. Special searches for new nearby dwarf galaxies have been undertaken Karachentsev et al. (2004). Also special cross-check has been done with IR and blind HI surveys (Karachentsev et al. 2007). The distances were measured from TRGB stars, Cepheids, the Tully-Fisher relation, and some other secondary distance indicators. Since the distances of galaxies in the Local Volume are measured independently of redshifts, we know their true 3D spatial distribution and their radial velocities. At present, the sample contains about 550 galaxies with distances less than 10 Mpc. A substantial fraction of the distances have been measured with accuracies as good as 8-10% (Karachentsev et al. 2004).

Within the Local Volume dwarf systems have been observed down to extremely low luminosities. This gives us a unique chance to detect voids, which may be empty of rather faint galaxies. Tikhonov & Karachentsev (2006) and Tikhonov & Klypin (2009) analyzed nearby voids. Here we use the same observational data as in Tikhonov & Klypin (2009) - the updated Catalog of Neighboring Galaxies (Karachentsev et al. 2004, private communication). We analyze a volume-limited sample of galaxies with absolute magnitudes $M_B < -12$ within 8 Mpc radius. The overall completeness of the sample has been discussed in Tikhonov & Klypin (2009).

3.1 Circular vs. rotational velocity

In order to compare results from an observational galaxy sample with dissipationless N-body simulations one has to assume certain hypotheses about how galactic properties are related with their host dark matter halos and, in particular, how the observed rotational velocity of a galaxy is related to the circular velocity of its dark matter halo.

A number of different techniques has been developed to associate galaxies with simulated DM haloes. The most well known techniques are the semi-analytical models (see the review of Baugh (2006)). An alternative approach is based on the conditional luminosity function (van den Bosch et al. 2004). Based on the merging history of the DM haloes and a set of physically motivated recipes the semi-analytical models place galaxies into the DM haloes. A number of free parameters of these recipes are calibrated by the observation of galaxies. A dark matter halo may host a luminous galaxy and a number of satellites. Although modern high resolution DM simulations resolve sub-haloes most of the semi-analytical models do not follow haloes which are accreted by larger ones but rather model the transformation of these

accreted satellites along their orbits. Recently, Maccio' et al. (2009) (see also Koposov et al. (2009)) claimed that semi-analytical models can solve the long standing problem of missing satellites (Klypin et al. 1999) within the Λ CDM scenario. The basic idea behind this solution of the problem is that the haloes which host a galaxy of a given measured rotational velocity are more massive than expected by the direct association of rotational velocity and the haloes maximum circular velocity. Since more massive haloes are less frequent the problem of missing satellites is solved. Thus it is solved at the expense of a predicted large population of dark satellites the observation of which remains another open problem in cosmology.

Stoehr et al (2002) were one of the first who argued that due to gravitational tides the total mass associated with dwarf spheroidals might be much larger than assumed. On the contrary, Kazantzidis et al. (2004) argue that tidal interaction cannot provide the mechanism to associate the dwarf spheroidals of the Milky Way with the massive substructures predicted by the Λ CDM model. Recently, Peñarrubia et al. (2008) analyzed the dynamics of the stellar systems in local group dwarf spheroidals and came to the conclusion that the associated dark matter circular velocity is about three times higher than the measured velocity dispersion of the stars.

All the previous arguments are mainly based on the assumption that the small galaxies under consideration are satellites of a more massive galaxy. However, in the analysis we report in this paper we will consider isolated dwarf galaxies for which these arguments are not necessarily valid.

In what follows we argue in favor of a direct association of the observed rotational velocity of a isolated dwarf galaxy to the maximum circular velocity of a simulated low mass DM halo. Our arguments are based on the comparison of the beam size of the observations with theoretical profiles of the DM haloes.

The Karachentsev et al. (2004) galaxy catalog contains for many of its galaxies the 21 cm HI line width at the 50% level from the maximum (W_{50}) as well as the apparent axial ratio (b/a). Using these informations Tikhonov & Klypin (2009) estimated the rotational velocity of the galaxy as $V_{\text{rot}} = W_{50}/2\sqrt{1 - (b/a)^2}$. They argue that a large fraction of the HI line width is likely produced by random motion of the order of 10 km s^{-1} but did not subtract those random motions. Their conclusions were based on a comparison of this rotational velocity with the circular velocities of the haloes. We follow their suppositions and associate the rotational velocity V_{rot} with the peak circular velocity of the dark matter halo. In order to give additional arguments in support of this assumption we compare now circular velocity profiles of dark matter haloes with the HI radius within which the observations are performed.

In Figure 4 we plot the NFW velocity profiles up to $4R_s$ for 7 haloes with masses between $5 \times 10^8 h^{-1} M_\odot$ and $2 \times 10^{10} h^{-1} M_\odot$. Here, we assumed concentrations following the fitting formula provided by Neto et al. (2007) which is in agreement with Macciò et al. (2007). Now we want to compare these circular velocities with the measured rotational velocities of nearby dwarfs. We use the FIGGS galaxy survey Begum et al. (2008) with $M_B > -14.5$ which is located inside the Local Volume. In this survey, measurements of W_{50} together with the HI diameters at a column density of $\approx 10^{19} \text{ atoms cm}^{-2}$ and the inclinations of optical images

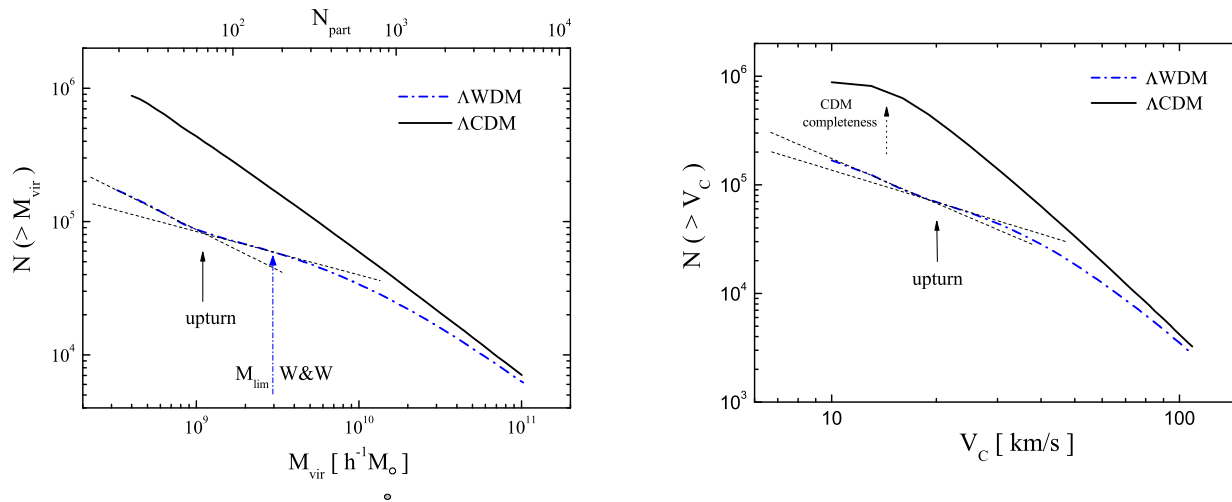


Figure 3. The AHF cumulative halo mass functions at redshift $z = 0$ (left) and the corresponding velocity function (right) for the Λ CDM (solid line) and Λ WDM (dashed-dotted line) simulations. The two dotted lines indicate the behavior of the mass function (velocity function) for haloes which are very likely fakes and those which should be real ones. We mark the intersection point as the mass limit below which fake and real haloes are mixed in the WDM simulation. For comparison, we also indicate the value for this mass limit calculated according to Wang & White (2007).

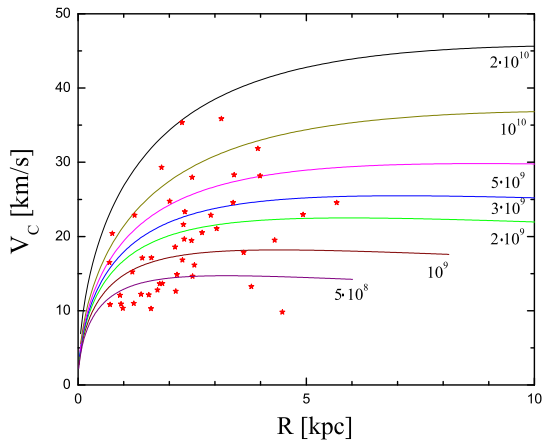


Figure 4. NFW circular velocity profiles for DM haloes with masses between $5 \times 10^8 h^{-1} M_{\odot}$ and $2 \times 10^{10} h^{-1} M_{\odot}$. Red stars: observed V_{rot} vs HI diameters taken from the FIGGS LV galaxy sample.

(i_{opt}) are provided. We estimated the rotational velocities as $V_{rot} = W_{50}/(2 \times \sin(i_{opt}))$ for galaxies with $i_{opt} > 40^\circ$ and plotted them vs. the HI radii on top of the NFW profiles in Figure 4.

One can clearly see that most of the observational points are located on the flattening parts of the NFW velocity profiles with circular velocities below 30 km s^{-1} . Since dwarf galaxies are expected to be dark matter dominated, the association of the observed rotational velocities at the HI radius with the maximum circular velocity of DM haloes is in our opinion a valid approximation.

4 VOID FINDER

Clusters, filaments and voids constitute the main components of the large-scale structure of the Universe. Soon after the discovery of the first cosmic void in the Boötes constellation (Kirshner et. al. 1981) it became clear that voids in galaxy distribution are the natural outcome of gravitational instability (Peebles 1982; Hoffman & Shaham 1982). During the last two decades the void phenomenon has been discussed extensively both from a theoretical as well as an observational point of view (see e.g. Peebles (2001)). There are many different possibilities to detect voids. A thorough review and comparison of different algorithms of void finders has been recently presented in Colberg et al. (2008). The void finders can be classified according to the method employed. Most are based on the point distribution of galaxies or DM haloes and some on the smoothed density or potential fields. Some of the finders are based on spherical filters while others assume no inherent symmetry and consider voids a crucial component of the cosmic web (e.g. Forero-Romero et al. (2008)).

Our void finder detects empty regions in a point distribution. These regions are not necessarily spherical. Our method is not sensitive to the total number of objects since the objects are mostly located in high density regions. But it is very sensitive to the appearance of objects in low density regions. In fact, any object detected in the middle of a void would divide it into two voids. A detailed description of the algorithm can be found in Tikhonov & Karachentsev (2006). Our void finder is somewhat similar to that used by El-Ad & Piran (1997) and Gottlöber et al. (2003). Namely, we place a 3D mesh on the observational or simulated sample. On this mesh, the identification of voids starts with the largest one. At first, we search for the largest empty sphere within the considered volume. The voids are supposed to be completely inside the geometric boundaries of the sample,

therefore, for a given grid point the radius of the largest empty sphere is determined by the minimum of the distance to the nearest galaxy (or halo) and the distance to the boundary of the sample.

The consecutive search for empty seed spheres with decreasing radius, R_{seed} , is combined with their subsequent expansion by means of addition of spheres whose centers are located inside the given void and whose radius is $R_1 > k \cdot R_{\text{seed}}$ where we assume $k = 0.9$. Thus, the spheres added to the void intersect with it by more than 30% of the volume. At any search step for an empty seed sphere, all previously identified voids are taken into account, i.e. void overlapping is not allowed. The search for voids continues as long as R_{seed} is larger than a threshold of 0.5 Mpc. This algorithm is simple, flexible and appropriate for our definition of voids as regions completely free from galaxies of certain luminosities.

With our assumption, $k = 0.9$, the voids adequately represent the empty regions between galaxies and at the same time preserve a sufficiently regular (elliptical) form. For $k = 1$, voids would be strictly spherical. When k decreases, the voids begin to penetrate into smaller and smaller holes, and the shapes of voids become more irregular. Assuming a very small k , one single void (the first one) would fill most part of the sampled volume. The value of the coefficient $k = 0.9$ used in this paper is a compromise, chosen after empirical detection of voids in distributions of points with different properties. The voids turn out to be well separated one from another and they can be approximated by triaxial ellipsoids.

Once we have identified the voids, we calculate the cumulative void function (VF) of their volumes. We applied also a spherical variant ($k = 1$) of our void finder and found that the assumption of sphericity of voids does not affect our results.

5 RESULTS

5.1 Local Volumes in the simulations

In the following we use the same criteria as Tikhonov & Klypin (2009) to select ‘‘LV-candidates’’ from our simulations. These are spheres of radius 8 Mpc which are characterized by the main features of the observed Local Volume galaxy sample. In our simulations the LV-candidates must be centered on a DM-halo with virial mass in the range $1 \times 10^{12} M_{\odot} < m_{\text{vir}} < 3 \times 10^{12} M_{\odot}$. This is our definition of a Local Group candidate. We do not require that this local group consists of two haloes comparable in mass because the appearance of two haloes instead of one halo of the same total mass does not change the dynamics of matter outside the Local group. We also do not require that the Local group should be at the same distance from a Virgo-type cluster as the observed one. Instead, we impose an overdensity constraints on the distribution of mass in the LV, which we take from the observed LV sample of galaxies. Below we summarize the conditions, which were used to find Local volumes in our simulations:

(i) We put a sphere of radius 8 Mpc on a Local group candidate.

(ii) No haloes with $m_{\text{vir}} > 2 \times 10^{13} M_{\odot}$ are inside this sphere.

(iii) There are no haloes more massive than $5.0 \times 10^{11} M_{\odot}$ in a distance between 1 and 3 Mpc.

(iv) The centers of the spheres (the Local Group candidates) are located at distances larger than 5 Mpc one from the other.

(v) The number density of haloes with $V_c > 100 \text{ km s}^{-1}$ inside this sphere exceeds the mean value in the whole box by a factor in the range 1.4 – 1.8.

We found 14 LV-candidates in the Λ WDM simulation which fulfill these criteria and 9 in the Λ CDM simulation. The reason for the difference is the tight requirement on the number density of massive halos. This means that in total between 18 and 23 massive halos must be in this sphere. Thus small differences between the position of a halo or its circular velocities in the Λ CDM and Λ WDM simulations may already lead to a violation of this criterion. Since the large scale structure in both simulations is quite similar we decided to use in the Λ CDM simulation the same LV-candidates as in the Λ WDM simulation. All these LV-candidates fulfill the first four criteria, 7 fulfill also the overdensity criterion, 5 are 10 % above or below (what is equivalent to 2 additional or missing halos with $V_c > 100 \text{ km s}^{-1}$) and two miss 5 halos. However, all these five halos are in the range $90 \text{ km s}^{-1} < V_c < 100 \text{ km s}^{-1}$. The advantage of our choice is that we can compare the properties of the same regions with the same large scale environment in both simulations.

Halo finders like FOF or AHF can find haloes down to 20 particles, however to determine the internal properties of haloes one needs much more particles. Moreover, the sample is not necessarily complete down to 20 particles per halo. There is a large scatter in the V_c vs. N_{part} relation which reduces substantially if one considers only isolated haloes. Haloes with $N_{\text{part}} \sim 100$ have circular velocities of $V_c \sim 20 \text{ km/s}$. In our simulation this limit coincides with the upturn of WDM velocity-mass function due to fake haloes. As an example for the existence of fake haloes in Λ WDM simulations Figure 5 shows the same LV-candidate in both models: top row for Λ WDM bottom row for Λ CDM. In the top, right plot one can clearly see filaments of regularly aligned spurious fake-haloes which extend across the voids and decrease their sizes. These are haloes with very low circular velocities. In the top left plot we have marked haloes with $15 < V_c \leq 20 \text{ km s}^{-1}$ by crosses and halos with $V_c > 20 \text{ km s}^{-1}$ by filled circles. One can clearly see the difference to the right plot: Haloes with $V_c \geq 20 \text{ km s}^{-1}$ (filled circles in the left plot) do not appear at all in artificial chains. Haloes with $15 < V_c \leq 20 \text{ km s}^{-1}$ only slightly modify the overall distribution and do not fill voids. Thus, they do not change substantially the void statistics. We did not find any such artificial regular filament of tiny haloes when we consider only halos above our limit of reliability $V_c = 20 \text{ km/s}$. We conclude that our analysis is not likely to be affected by spurious haloes as long as we consider halo samples with circular velocities $V_c > 20 \text{ km s}^{-1}$ and might be slightly affected for samples with $V_c > 15 \text{ km s}^{-1}$.

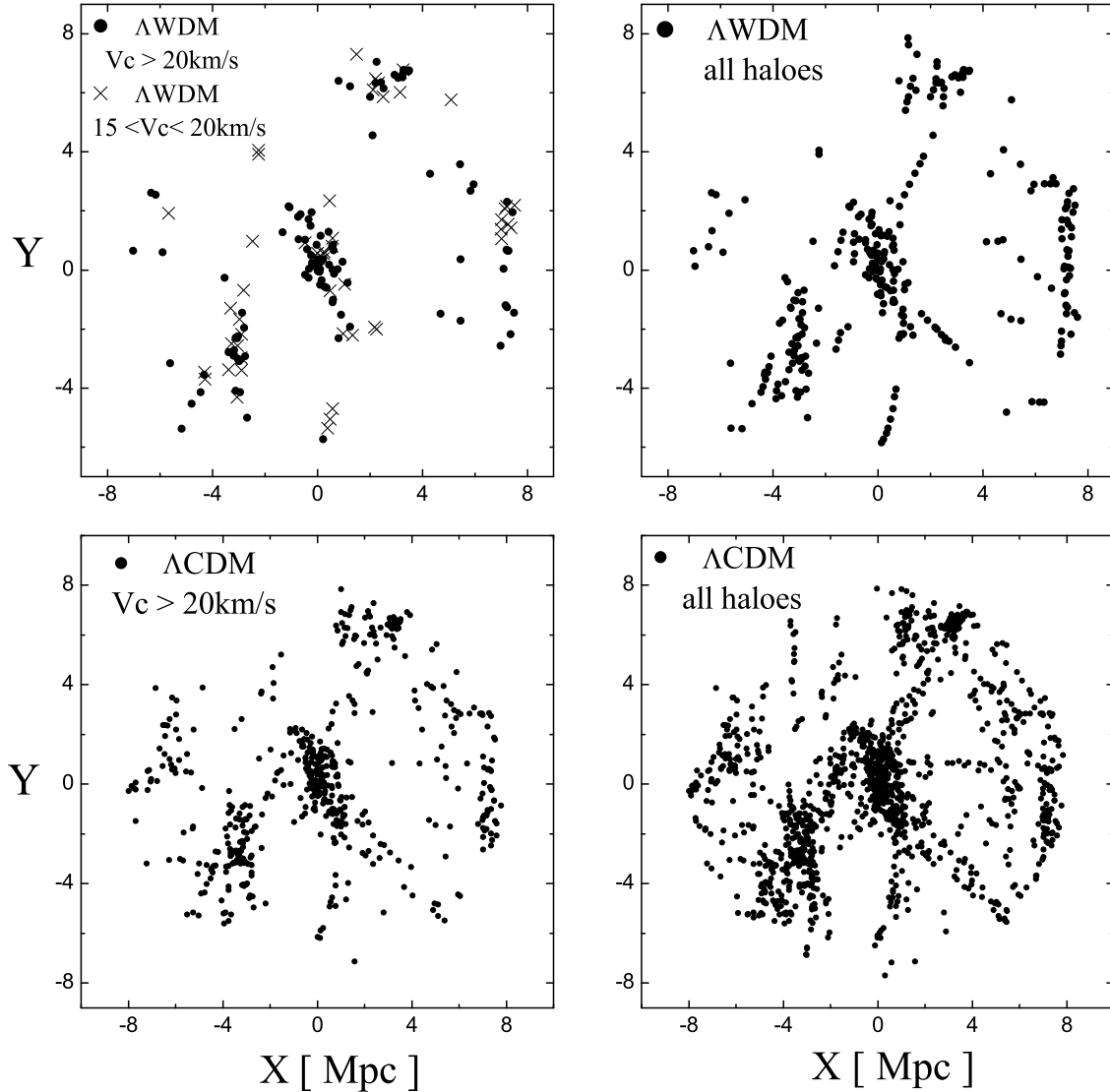


Figure 5. Distribution of haloes in a slice of 4 Mpc thickness through the center of an LV-candidate. The upper panel shows the Λ WDM model, on the left plot haloes with $V_c \geq 20 \text{ km s}^{-1}$ are marked by filled circles and haloes with $15 < V_c < 20 \text{ km s}^{-1}$ by crosses. On the right plot all haloes are shown. The lower panel shows the distribution of the corresponding Λ CDM haloes.

5.2 Properties of voids

The Local Volumes contain a large number of mini-voids with radii R_v smaller than about 4 Mpc. We characterize these mini-voids by the cumulative volume of the mini-voids $V_{\text{void}}(R > R_v)$ normalized to the Local Volume V_{LV} . In Figure 6 we compare the cumulative volume filling fraction (VFF) of mini-voids ($V_{\text{void}}(R > R_v)/V_{\text{LV}}$) of the 14 LVs found in the Λ WDM simulation with the observed VFF for $M_B < -12$ galaxies. The figure indicates that the VFF in the distribution of haloes with $V_c > 20 \text{ km s}^{-1}$ fits well to

the observed one. In fact, the observed spectrum of local mini-voids is reproduced within the Λ WDM model almost over the full range of void volumes. The size of the large voids reduces slightly if we assume that haloes with $V_c > 15 \text{ km s}^{-1}$ define the voids. With the present mass resolution we cannot exclude that this reduction is due to fake haloes. In the luminosity range $-13.2 < M_B < -11.8$ only three field galaxies have been observed with $V_{\text{rot}} < 15 \text{ km s}^{-1}$ (table 3 of Tikhonov & Klypin (2009)). So far, the existence of such very slowly rotating (low mass) galaxies is not in contradiction with the assumption of WDM.

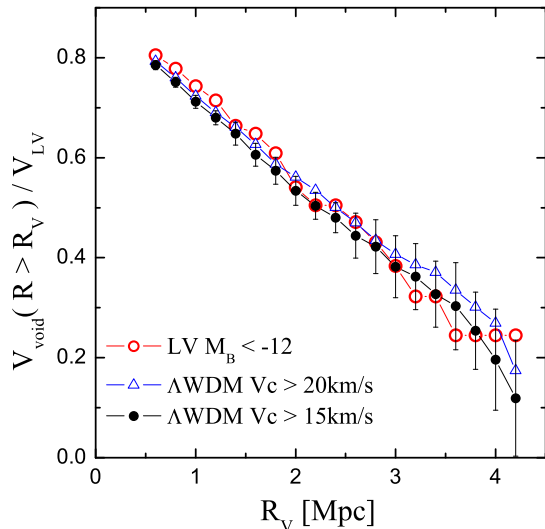


Figure 6. Volume fraction of the LV occupied by mini-voids (VFF). The VFF of the observational sample with $M_B < -12$ (red circles) is compared with the mean VFF obtained from the 14 LVs in the Λ WDM simulation with haloes with circular velocity $V_c > 20 \text{ km s}^{-1}$ (open blue triangles) and $V_c > 15 \text{ km s}^{-1}$ (filled black circles), for which the 1σ scatter is also shown.

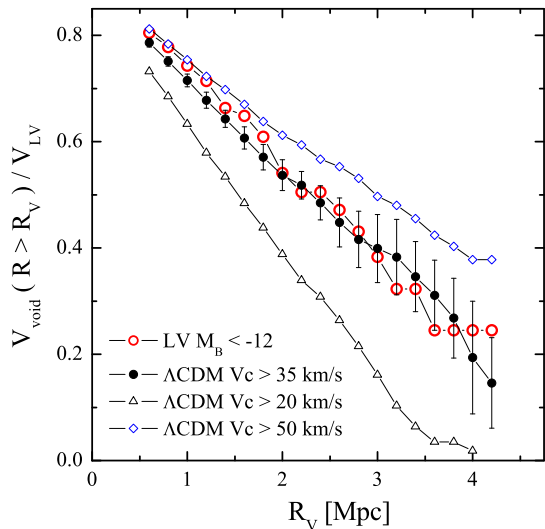


Figure 7. Volume fraction of the LV occupied by mini-voids (VFF). The VFF of the observational sample with $M_B < -12$ (red circles) is compared with the mean VFF obtained from the 14 LVs in the Λ CDM simulation with haloes with circular velocity $V_c > 20 \text{ km s}^{-1}$ (open triangles), $V_c > 50 \text{ km s}^{-1}$ (open diamonds), and $V_c > 35 \text{ km s}^{-1}$ (filled black circles), for which the 1σ scatter is also shown.

The VFF obtained from the Λ CDM simulation matches observations only if we assume that objects with $V_c > 35 \text{ km s}^{-1}$ define the local mini-voids (Figure 7). The Λ CDM VFF is well above the data, if we assume $V_c > 50 \text{ km s}^{-1}$ for the void definition and it is far below the observational data if we assume $V_c > 20 \text{ km s}^{-1}$, i.e. in this case large mini-voids are missing in the numerical realizations of local volumes. Thus, our Λ CDM simulation is in agreement with observational data if haloes with $V_c < 35 \text{ km s}^{-1}$ do not host any galaxy. This statement is independent of the volume under consideration. As a test of reliability we repeated the VFF analysis assuming a LV of radius 6 Mpc both in observations and in our 14 simulated LVs. We recovered the same circular velocity $V_c \approx 35 \text{ km s}^{-1}$ for haloes hosting galaxies with $M_B < -12$. Thus we are sure that our original sample is not influenced by voids which intersect the outer bound of the LV.

However, a significant amount of LV galaxies with magnitudes $M_B \sim -12$ and rotational velocity as low as $V_{rot} \lesssim 20 \text{ km s}^{-1}$ have been recently observed. A systematically selected sample of such extremely faint nearby dwarf irregular galaxies has been observed with the Giant Metrewave Radio Telescope (Begum et al. 2008). Dwarf irregulars are typically dark matter dominated. These objects have surprisingly regular kinematics. One of the faintest ones is Camelopardalis B with $M_B \sim -10.9$ (Begum, Chengalur & Hopp 2003).

Within the Λ CDM model mini-voids with sizes $R_V > 1$ Mpc cover a volume of about 1600 Mpc^3 (or about 75 % of the sample volume, see Figure 7). We found a mean of 463 ± 85 haloes with $20 < V_c < 35 \text{ km s}^{-1}$ within the mini-voids of a simulated LV where the scatter is the 1σ fluctuation between the 14 LVs. This number is more than an order of magnitude above the observed number of faint galaxies in the Local Volume. Thus the Λ CDM model fails to explain the observed local VFF. The predicted overabundance of low-mass galaxies in low density regions is similar to another problem well known in high density regions where the Λ CDM model predicts an order of magnitude overabundance of low-mass satellites. Typically the more massive haloes ($30 < V_c < 35 \text{ km s}^{-1}$) can be found near the borders of the mini-voids whereas the smallest ones tend to be in the center. A similar behavior has been found in large voids (Gottlöber et al. 2003).

5.3 RMS peculiar velocities

Next, the Hubble flow around the LG-like objects is studied in an attempt to confirm that our LV-candidates are indeed the numerical counterparts of the observed LV. To this end, we calculated the rms radial velocity deviations from the Hubble flow, σ_H , both for the observational data and the objects in the simulated LVs. As limits of circular velocities of haloes used in our analysis, we took the values found from the previous void analysis. We used haloes with circular velocities $V_c > 20 \text{ km s}^{-1}$ in the Λ WDM and with $V_c > 35 \text{ km s}^{-1}$ in the Λ CDM sample. But even if we assume for the Λ CDM sample the lower value of $V_c > 20 \text{ km s}^{-1}$ the result does not change substantially in spite of the significant increase in the number of objects.

Following Tikhonov & Klypin (2009) we calculate σ_H in the rest frame of the considered galaxy sample, i.e. we correct for the apex motion. We correct the rms velocities

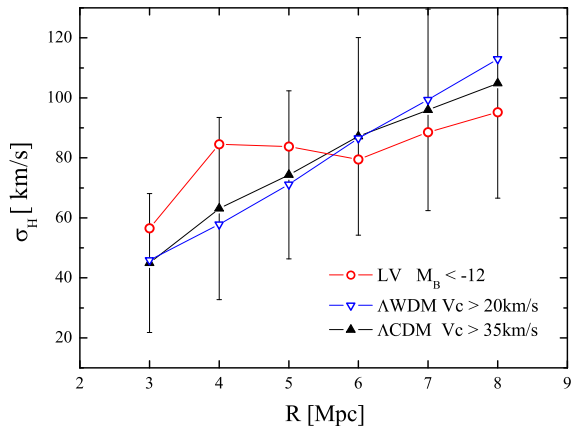


Figure 8. The rms radial velocity deviations from the Hubble flow σ_H for galaxies with $M_B < -12$ in the Local Volume with distances from 1 Mpc up to R (red curve with open circles). The estimates are corrected for the apex motion and for distance errors. Black filled triangles with error bars show the mean σ_H on corresponding scales for 14 CDM LV-candidates for haloes with $V_c > 35 \text{ km s}^{-1}$ with $1\text{-}\sigma$ scatter. Blue triangles - mean σ_H for WDM LV-candidates for haloes with $V_c > 20 \text{ km s}^{-1}$.

of the galaxies also for distance errors. Depending on radius these corrections reduce the value of σ_H by about 5% to 15% (cf. Table 3 of Tikhonov & Klypin (2009)). Figure 8 shows the observed σ_H in the range from 1 Mpc to R and the mean value obtained around the Local Group in the center of each of the 14 LVs in the Λ CDM and Λ WDM simulations. In Fig. 8 we compare the σ_H of our numerical LVs with the observed one and found a reasonable agreement for both models. We error bars show the scatter among the 14 LVs of the Λ CDM model. In Λ WDM we found about the same scatter. The excess seen in the observed σ_H at $R = 4$ and 5 Mpc probably reflects the fact that most of the galaxy groups of the LV are located within a distance of 3 to 5 Mpc from our Local Group. They are responsible for the corresponding overdensity at these distances. However, we did not include this constrain when we searched for LV-candidates in simulations for the sake of having better statistics. Not surprisingly, the results found from the Λ CDM and Λ WDM LVs agree pretty well among them and with data.

Peculiar motions on the scale of a few Mpc reflect the mass distribution on these scales and larger ones, hence they should not be affected by the small scale damping of the primordial perturbations. We conclude that there is no difference between the two cosmologies in terms of the internal dynamics of these systems, in good agreement with other works (Martinez-Vaquero et.al 2009).

6 FORMING GALAXIES IN HALOES

As we mentioned above, very faint low-mass galaxies have been observed in the local universe with rotational velocities below 20 km s^{-1} . As an example, Camelopardalis B with $M_B \sim -10.9$ has a total dynamical mass of $\approx 10^8 h^{-1} M_\odot$

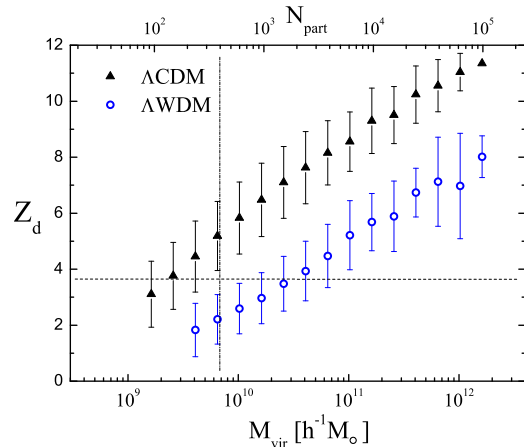


Figure 9. Redshift z_d at which the progenitors of present day LV haloes became more massive than $3 \times 10^8 h^{-1} M_\odot$ as a function of present day virial mass (upper axis: number of particles in the halo). Filled triangles: Λ CDM model, open circles: Λ WDM model. Dashed lines: see text.

measured at the last point of the observed rotation curve (Begum, Chengalur & Hopp 2003). Due to the strong bias between dark haloes and galaxies, it is not easy to compare these observations with collisionless N-body simulations. A proper way of doing it would be by means of full hydrodynamical simulations which includes all the relevant physical processes that lead to the formation of galaxies inside the dark matter potentials. Nevertheless, we can use results from such kind of simulations to derive estimates on the formation epochs of the galaxies that would form in the dark haloes of our simulated local volumes. Hoesft et al. (2006) have simulated the formation and evolution of dwarf galaxies in voids using high resolution Λ CDM hydrodynamical simulations which include radiative cooling, UV photoionization from a cosmic background, star formation from the cooled gas and feedback from supernovae. Based on these simulations, they derived a characteristic mass scale $M_c(z)$ below which UV photoheating suppresses further cooling of gas and therefore star formation inside haloes with $M < M_c(z)$. The numerical results can be well approximated by an exponentially decreasing function with redshift in the following way

$$\frac{M_c(z)}{10^{10} h^{-1} M_\odot} = \frac{0.62}{(1+z)^{1.23} \exp(0.082z^{2.1})} \left\{ \frac{\Delta_c(0)}{\Delta_c(z)} \right\}^{1/2} \quad (1)$$

where $\Delta_c(z)$ represents the redshift dependence of the characteristic virial overdensity of halos that can be obtained from the numerical integration of the equations of the spherical infall model or using the analytical approximation obtained by Bryan & Norman (1998).

Thus, by comparing the mass of the progenitors of each of our LV haloes with $M_c(z)$ we can estimate the typical formation redshift for the galaxies in our LV's. Those haloes with mass accretion histories that are always above $M_c(z)$ have been able to form stars at all times. On the contrary, those haloes with mass accretion histories shallower than $M_c(z)$ would have not been able to condense baryons inside and they would not host any galaxy. Although these results were obtained for Λ CDM halos, in what follows, we

will assume that they can be applied also to our Λ WDM simulations. Since the UV photionization background comes from observations and the modeling of the rest of the other baryonic processes is the same, the only differences between the Λ CDM and Λ WDM halos would come from the different mass accretion histories.

The "age" of an object in simulations is often determined as the epoch at which half of its mass is gathered. Thus massive objects form later. Contrary to this definition of formation time, there are others such as the time at which progenitors of present day haloes reach a given mass threshold. In numerical simulations a natural threshold is given by the mass resolution which defines a minimum halo mass as the detection limit. Obviously, more massive objects reached earlier a given mass threshold and thus, they have formed earlier, according to this definition of formation time. Here we use the detection limit as an estimate for the formation time of the haloes in the simulation and compare the evolution of Λ CDM and Λ WDM haloes after passing this threshold which we take to be the mass corresponding to a minimum of 20 particles (i.e. $3.2 \times 10^8 h^{-1} M_\odot$). For the cosmological parameters under consideration the characteristic mass scale, $M_c(z)$ equals this mass resolution limit for haloes in our simulations at redshift $z = 3.7$ and increases up to $6.2 \times 10^9 h^{-1} M_\odot$ at redshift $z = 0$. Therefore, we are interested to determine at which redshift z_d the most massive progenitor of the redshift zero LV haloes reaches the mass threshold ($3.2 \times 10^8 h^{-1} M_\odot$) of our simulations. To this end, we identify with an FOF analysis all the progenitors of a given halo at different redshifts.

In Figure 9 we show the mean redshift z_d as a function of the present day halo's virial mass for all haloes found in the 14 LVs of the Λ CDM and Λ WDM model. We consider that for Λ CDM haloes with more than 100 particles, their merging history can easily be followed. In the case of Λ WDM we restrict ourselves to haloes above the limiting mass M_{lim} (see §2). The symbols are centered in the middle of the selected mass bins and the error bars show the 1σ scatter. The difference between the two models is evident: there is a general trend for Λ WDM haloes of all masses to reach this threshold later than the Λ CDM ones.

The dashed vertical line in Figure 9 marks the characteristic mass for redshift zero, $M_c(0) = 6.2 \times 10^9 h^{-1} M_\odot$. More massive haloes would have formed stars all their lifetime because their mass accretion histories are always above the $M_c(z)$ since z_d till present. Those haloes with present day masses below this characteristic mass would be at present practically devoid of gas due to UV photoheating. Within the Λ CDM model the characteristic, M_c , mass increases faster with time than the mean halo mass. Therefore, the mass of those haloes was at some earlier redshift larger than $M_c(z)$ and thus the haloes were able to form stars in the past.

The horizontal dashed line in Figure 9 marks the redshift $z^* = 3.7$ at which $M_c(z^*) = 3.2 \times 10^8 h^{-1} M_\odot$ (the resolution limit). The redshift of the first identified progenitor of Λ CDM haloes with $M_{vir} > 2.2 \times 10^9 h^{-1} M_\odot$ is always above this line. Therefore, all these haloes have been able to cool gas and form stars at least until redshift 3.7. Those with masses $M > M_c(0)$ will have formed stars up to present. The smaller haloes, with $M < M_c(0)$ would have formed stars only until $M_c(z)$ became larger than the

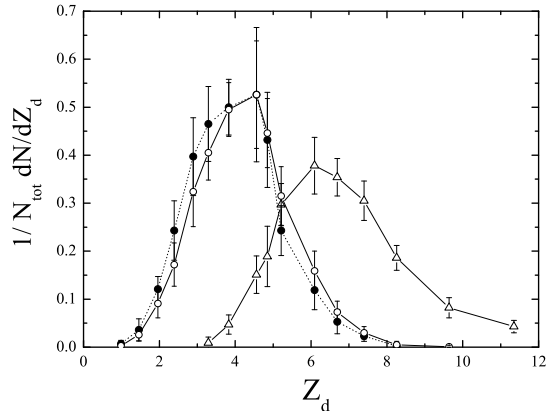


Figure 10. The differential number fraction $\frac{1}{N_{tot}} \frac{dN}{dz}$ of progenitors of haloes which became more massive than $3 \times 10^8 h^{-1} M_\odot$ at redshift z_d . Filled circles: haloes with $V_c < 35 \text{ km s}^{-1}$ at $z = 0$ inside mini-voids, open circles: haloes with $V_c < 35 \text{ km s}^{-1}$ outside mini-voids, triangles: haloes with $V_c > 35 \text{ km s}^{-1}$. Error bars are 1σ deviations.

progenitors halo mass (somewhere between z_d and present). Haloes with $M_{vir} < 2.2 \times 10^9 h^{-1} M_\odot$ lost most of their gas before $z^* = 3.7$. Therefore, they can host only an old population of stars.

In sharp contrast with the Λ CDM case, the Λ WDM haloes with $M_{vir} < M_c(0)$ are always below the horizontal dotted line. Thus their mass was always smaller than $M_c(z)$ and they were unable to condense baryons and form galaxies at all. This points towards a potential problem of the Λ WDM model, namely an insufficient formation of dwarf galaxies. Since $M_c(z)$ drops down very fast for $z > 4$, in principle they could have been able to cool gas and form stars at earlier times, resulting in a population of faint red dwarfs.

Since haloes form much later in the Λ WDM scenario they can lose their gas much easier due to the photoheating of the cosmic ionizing background than the Λ CDM haloes of the same present day mass. Therefore, the formation of a sufficient number of low mass galaxies could be a problem in this model. To study this in full detail, one needs to perform Λ WDM simulations with much higher mass resolution than the one presented here.

In Figure 10 we compare the formation history of Λ CDM haloes with circular velocities $V_c < 35 \text{ km s}^{-1}$ located inside the mini-voids (filled circles) with haloes in the same range of circular velocities, but located outside the voids (open circles). We show the differential number fraction $\frac{1}{N_{tot}} \frac{dN}{dz}$ of progenitors of haloes which became more massive than $3.2 \times 10^8 h^{-1} M_\odot$ at redshift z_d which has the same meaning as in Fig. 9. We used haloes with masses $M > 2 \times 10^9 h^{-1} M_\odot$. Therefore, the mean z_d of Fig. 10 corresponds to the second filled triangle of Fig. 9. As can be seen in the figure, regardless of environment, these haloes have very similar formation histories. For comparison, we also show the results for the more massive haloes in the LVs (triangles: $V_c > 35 \text{ km s}^{-1}$) which obviously passed much earlier the threshold z_d . The fact that we do not see strong

differences in the formation epochs of dwarf haloes located in structures and those sitting in voids may have profound consequences for the Λ CDM model.

One of the proposed scenarios to solve the overabundance problem assumes that UV-photoionization evaporates gas from dwarf haloes in voids and therefore quenches star formation and leaves voids empty. If, however, dwarf haloes in voids and the surrounding structures form roughly simultaneously then photoionization should have suppressed the formation of all these dwarf galaxies regardless of environment. As shown above the Λ CDM model predicts an order of magnitude more low-mass haloes than observed. If photoionization suppresses the formation of galaxies in more than 90 % of the small haloes, it is difficult to explain why none of the remaining is found in the voids. Therefore, the observed small number of dwarfs represents a similar problem for the Λ CDM model as the missing satellites.

However, the observed dwarfs could also be a potential problem for the Λ WDM model. According to the late formation time of the small mass haloes they spend almost all their lifetime having masses well below the characteristic mass $M_c(z)$. Following the arguments of Hoefl et al. (2006) it would be difficult to explain how they could have formed stars at all. However, we should also note that the characteristic mass has been derived based on Λ CDM simulations (Hoefl et al. 2006; Okamoto, Gao, & Theuns 2008). To get a final answer for halos in the WDM scenario, proper gas-dynamical simulations including star formation should be performed. Such simulations should have extremely high resolution to address also the problem of fake halo formation.

7 DISCUSSION AND CONCLUSIONS

We used an updated version of the Karachentsev et al. (2004) sample of galaxies to compare the distribution and motions of galaxies in the Local Volume with that of dark matter haloes in Λ CDM and Λ WDM simulations. About 40 mini-voids with sizes in the range from 0.5 Mpc to 4 Mpc have been detected in the observational sample. Tikhonov & Klypin (2009) have shown that the spectrum of void sizes is stable with respect to variations of the sample and to uncertainties of distances to individual galaxies.

From our Λ CDM and Λ WDM simulations we have selected the Local Volume candidates following the criteria used by Tikhonov & Klypin (2009). In many respects these LV-candidates look very similar to the observed Local Volume: they have comparable number of bright (massive) objects and a similar density contrasts on 8 Mpc scale. Moreover, most of the LV-candidates show the same typical intersecting filaments sometimes nearly aligned in planes which are quite similar to what one observes in the Local Volume - intersecting filaments form a structure which is part of the Local Supercluster and goes through the Local Group (sometimes it is called "Local Sheet"). The 14 Local Volume candidates in Λ CDM and Λ WDM simulations show only little scatter in the volume fraction occupied by mini-voids. Thus it is well suited to discriminate between different models. To test further our LV-candidates we have calculated the rms radial velocity deviations from the Hubble flow and found no difference in the dynamics of the haloes. Both in

the Λ CDM and Λ WDM models σ_H is in agreement with the observations.

In Sect. 3.1 we argue in favor of an association of the haloes maximum circular velocity to the observed rotational velocity. Our argument is based on a comparison of the rotational velocities observed in a certain distance from the center and the circular velocities of dark matter haloes in the same distance. The velocity profiles of the dark matter haloes in are essentially flat at the distance where the rotational velocities of dwarfs are measured. Thus the errors are small if one associates the measured rotational velocity to the peak circular velocity. The exact relation between both depends on the gasdynamical processes in the galaxy which we cannot consider in the large volume under discussion. One might argue that the peak velocity increases due to adiabatic contraction so that the WDM model would be even more favored. However, these dwarf haloes are expected to be dark matter dominated and adiabatic contraction is expected to be less important. One might argue that by some processes the rotational velocity in the dwarf haloes becomes smaller but we cannot see a good reason to associate V_{rot} with significantly more massive haloes which would be necessary to fit the observational data.

Within the Λ CDM model the cumulative volume fraction of the LV occupied by mini-voids matches observations only if one assumes that objects with $V_c > 35 \text{ km s}^{-1}$ define the local mini-voids and these objects host galaxies brighter than $M_B = -12$ (Tikhonov & Klypin 2009). The Λ CDM model predicts almost 500 haloes with $20 < V_c < 35 \text{ km s}^{-1}$ within the mini-voids in a LV. At present 10 quite isolated dwarf galaxies have been observed in the Local Volume with magnitudes $-11.8 > M_B > -13.3$ and rotational velocities $V_{rot} < 35 \text{ km s}^{-1}$ (Tikhonov & Klypin 2009). This number is more than an order of magnitude smaller than the predicted number of low-mass haloes and thus it points to a similar discrepancy as the well known predicted overabundance of satellites in Milky Way sized Λ CDM haloes. The reason can be understood from the Λ CDM mass function at the low-mass end which is much steeper than the observed luminosity function at the low luminosity end. This causes both the overabundance of satellites and the fact, that the observed mini-void distribution can be explained only if haloes with circular velocities larger than 35 km s^{-1} host galaxies. In case of satellites one could explain the mismatch between observations and predictions by processes like ram-pressure and tidal stripping which have not been taken correctly into account in simulations. On the contrary, the dwarfs in the Local Volume are all situated in the same environment of relatively low density. Therefore, the existence of only a small number of such low luminosity and low mass dwarf galaxies in the LV is even more difficult to explain than the missing satellites.

In case of the Λ WDM model the observed spectrum of mini-voids can be explained naturally if dark matter haloes with circular velocities larger than $\sim 15 - 20 \text{ km s}^{-1}$ host galaxies. The observed small number of slowly rotating isolated galaxies is not in contradiction with this assumption since a small number of low-mass haloes are also formed in the Λ WDM model. Thus the Λ WDM model solves the problem of overabundance and the spectrum of mini-voids in a distribution of low-mass haloes is in agreement with observations. However, we have also shown that due to the

late formation of haloes in the Λ WDM model a substantial part, if not all, of the low-mass haloes could have failed to form stars. Thus they would have not been able to host any visible galaxy, as it is necessary for the model to agree with the sizes of mini-voids in the Local Universe. Nevertheless, to study their distribution and properties in detail one needs simulations with much higher resolution so that one can distinguish between the real low-mass haloes and the numerical artifacts. Moreover, full radiative hydrodynamical simulations with star formation are also needed in order to properly address the galaxy formation process in these halos. Overall we confirm earlier claims that concerning the formation of small scale structure the Λ WDM model can be considered as a promising alternative to the Λ CDM model. However, more detailed investigations are necessary to study to which extent star formation in low-mass haloes is suppressed in the Λ WDM model.

ACKNOWLEDGMENTS

We thank I.D. Karachentsev for providing us with an updated list of his Catalog of Neighboring Galaxies. The simulations used in this work were performed at the Leibniz Rechenzentrum Munich (LRZ) and at the Barcelona Supercomputing Centre (BSC), partly granted by the DEISA Extreme Computing Project (DECI) SIMU-LU. This work was funded by the Deutsche Forschungsgemeinschaft (DFG grant: GO 563/17-1) and supported by the ASTROSIM network of the European Science Foundation (ESF). SG acknowledges a Schonbrunn Fellowship at the Hebrew University Jerusalem. YH has been partially supported by the ISF (13/08). GY acknowledges support of the Spanish Ministry of Education through research grants FPA2006-01105 and AYA2006-15492-C03. We thank A. Klypin for useful discussions and suggestions.

REFERENCES

- Abazajian K., *Phys. Rev. D*, 73, 063513, (2006)
- Abazajian K., Koushiappas S. M., 2006, *PhRvD*, 74, 023527
- Avila-Reese V., Colín P., Valenzuela O., D’Onghia E., Firmani C., *ApJ*, 559, 516, (2001)
- Baugh C. M., 2006, *RPPh*, 69, 3101
- Begum A., Chengalur J. N., Karachentsev I. D., Sharina M. E., Kaisin S. S., 2008, *MNRAS*, 386, 1667
- Begum A., Chengalur J. N., Hopp U., 2003, *NewA*, 8, 267
- Bode P., Ostriker J. P., Turok N., 2001, *ApJ*, 556, 93
- Bryan G. L., Norman M. L., 1998, *ApJ*, 495, 80
- Colberg J. M., Pearce F., Foster C., Platen E., Brunino R., Neyrinck M., Basilakos S., Fairall A., Feldman H., Gottlöber S., Hahn O., Hoyle F., Müller V., Nelson L., Plionis M., Porciani C., Shandarin S., Vogeley M. S., 2008, *MNRAS*, 387, 933
- Colín P., Valenzuela O., Avila-Reese V., 2008, *ApJ*, 673, 203
- Crain R. A., Eke V. R., Frenk C. S., Jenkins A., McCarthy I. G., Navarro J. F., Pearce F. R., 2007, *MNRAS*, 377, 41
- H. El-Ad and T. Piran, *ApJ*, 491, 421 (1997)
- Forero-Romero J. E., Hoffman Y., Gottlöber S., Klypin A., Yepes G., 2008, arXiv, arXiv:0809.4135
- Gottlöber S., Lokas E. L., Klypin A., Hoffman Y., 2003, *MNRAS*, 344, 715
- Hoefl M. et al., *MNRAS*, 2006, 371, 401
- Hoffman Y., Ribak E., 1991, *ApJ*, 380, L5
- Hoffman Y., Shaham J., 1982, *ApJ*, 262, L23
- Karachentsev I.D., Karachentseva V.E., Huchtmeier W.K., Makarov D.I., 2004 *AJ*, 127, 2031
- Karachentsev I.D., Karachentseva V., Huchtmeier W., Makarov D., Kaisin S., Sharina M., Mining the Local Volume, 2007, arXiv:0710.0520
- Karachentsev et al., 2001, *A&A*, 379, 407.
- Kazantzidis S., Mayer L., Mastropietro C., Diemand J., Stadel J., Moore B., 2004, *ApJ*, 608, 663
- Kirshner R.P., Oemler A., Schechter P.L., Shectman S.A., 1981, *ApJ*, 248, L57
- Klypin A., Kravtsov A. V., Valenzuela O., Prada F., 1999, *ApJ*, 522, 82
- Knebe A., Devriendt J. E. G., Mahmood A., Silk J., *MNRAS*, 329, 813, (2002)
- Knollmann, S., & Knebe, A., *ApJS*, in press, (2009).
- Koposov S. E., Yoo J., Rix H.-W., Weinberg D. H., Macciò A. V., Escudé J. M., 2009, *ApJ*, 696, 2179
- Kraan-Korteweg R.C., Tammann, G.A., 1979, *Astronomische Nachrichten*, 300, 181
- Loeb A., 2008, arXiv:0804.2258
- Macciò A. V., Dutton A. A., van den Bosch F. C., Moore B., Potter D., Stadel J., 2007, *MNRAS*, 378, 55
- Macciò A. V., Kang X., Fontanot F., Somerville R. S., Koposov S. E., Monaco P., 2009, arXiv, arXiv:0903.4681
- Martinez-Vaquero, L.A., Yepes, G., Hoffman, Y. & Gottlöber, S., *MNRAS*, submitted, (2009)
- Miranda M., Macciò A. V., *MNRAS*, 382, 1225 (2007)
- Moore B., Ghigna S., Governato F., Lake G., Quinn T., Stadel J., Tozzi P., 1999, *ApJ Lett.*, 524, L19
- Neto A.F., Gao L., Bett P., Cole S., Navarro J.F., Frenk C.S., White S.D.M., Springel V., Jenkins A., 2007, *MNRAS*, 381, 1450
- Okamoto T., Gao L., Theuns T., 2008, *MNRAS*, 390, 920
- Peebles P. J. E., 1982, *ApJ*, 257, 438
- Peebles P. J. E., 2001, *ApJ*, 557, 495
- Peñarrubia J., McConnachie A.W., Navarro J.F., 2008, *ApJ*, 672, 904
- Spergel D. N., et al. 2003, *ApJS*, 148, 175
- Spergel D. N., et al. 2007, *ApJ Suppl.*, 170, 377
- Springel V., 2005, *MNRAS*, 364, 1105
- Steffen F. D., 2006, *JCAP*, 9, 1
- Stoehr F., White S.D.M., Tormen G., Springel V., 2002, *MNRAS*, 335, 84
- Tikhonov A.V., Karachentsev I.D., 2006, *ApJ*, 653, 969
- Tikhonov A. V., Klypin A., 2009, *MNRAS*, 395, 1915
- Tully R.B., Fisher J.R., 1987, *Atlas of Nearby Galaxies*, Cambridge University Press
- van den Bosch F. C., Norberg P., Mo H. J., Yang X., 2004, *MNRAS*, 352, 1302
- Viel M., Lesgourgues J., Haehnelt M. G., Matarrese S., Riotto A., *PhysRevD*, 71, 063534, (2005)
- Viel M., Colberg J. M., Kim T.-S., 2008, *MNRAS*, 386, 1285
- Viel M., Becker G. D., Bolton J. S., Haehnelt M. G., Rauch M., Sargent W. L. W., *Phys.Rev.Lett.*, 100, 041304, (2008)

Wang J., White S.D., 2007, *MNRAS*, 380, 93
Yepes G., Gottlöber S., Martínez-Vaquero L. A., Hoffman
Y., 2009, AIPC, 1115, 80
Yepes, G., et. al. in preparation, (2009)
Zavala J., Jing Y. P., Faltenbacher A., Yepes G.,
Hoffman Y., Gottlober S., Catinella B., 2009, arXiv,
arXiv:0906.0585, ApJ in print